



| | |
|--------------|--|
| Title | Fatigue performance of bonding-assisted fillet weld roots by inserting adhesive material |
| Author(s) | Jiahao, Mao; Hirohata, Mikihiro; Yifei, Xu et al. |
| Citation | Fatigue and Fracture of Engineering Materials and Structures. 2024, 47(10), p. 3646-3657 |
| Version Type | VoR |
| URL | https://hdl.handle.net/11094/98132 |
| rights | This article is licensed under a Creative Commons Attribution 4.0 International License. |
| Note | |

The University of Osaka Institutional Knowledge Archive : OUKA

<https://ir.library.osaka-u.ac.jp/>

The University of Osaka

Fatigue performance of bonding-assisted fillet weld roots by inserting adhesive material

Mao Jiahao¹  | Hirohata Mikihiro¹ | Xu Yifei¹ | Chang Kyong-Ho²

¹Department of Civil Engineering,
Division of Global Architecture, Graduate
School of Engineering, Osaka University,
Suita, Japan

²Department of Civil Environment &
Plant Engineering, Chung-Ang
University, Seoul, South Korea

Correspondence

Hirohata Mikihiro, 2-1, Yamada-oka,
Suita, Osaka 565-0871, Japan.
Email: hirohata@civil.eng.osaka-u.ac.jp

Abstract

This study proposes a novel method to prevent fatigue cracks at the root of fillet welds in steel bridge supports by inserting epoxy resin as an adhesive material. A total of 36 specimens, categorized into welded-only and bonding-assisted types, were subjected to a series of four-point bending fatigue tests to simulate cyclic tensile stress conditions. Additionally, finite element analysis was employed to investigate the impact of epoxy insertion on stress distribution near the weld root. The results demonstrated that bonding-assisted specimens exhibited significantly improved fatigue life compared to welded-only specimens, with a notable reduction in tensile stress at the weld root. Furthermore, a displacement-based method was employed to evaluate weld root fatigue performance, yielding consistent results. These findings highlight the potential of integrating adhesive bonding in fillet welds to improve the durability and service life of steel bridge structures by effectively mitigating fatigue-related issues.

KEYWORDS

bonding, fatigue, fillet welding, steel bridge, weld root

Highlights

- Preventing fatigue cracks in fillet weld root through epoxy insertion.
- Inserted rubber prevents welding defects caused by epoxy burning during welding.
- The combination of welding and bonding reduces the opening displacement of the weld root.
- Displacement-based method can effectively evaluate weld root fatigue life.

This is an open access article under the terms of the [Creative Commons Attribution](https://creativecommons.org/licenses/by/4.0/) License, which permits use, distribution and reproduction in any medium, provided the original work is properly cited.

© 2024 The Author(s). *Fatigue & Fracture of Engineering Materials & Structures* published by John Wiley & Sons Ltd.

1 | INTRODUCTION

In recent years, issues on the maintenance and management of bridges have gained increasing prominence. Given the extended service life expected of structures such as bridges, one of the paramount considerations is their durability. Regarding steel bridges, fatigue emerges as a critical concern, significantly influencing their long-term performance.^{1,2} Welded joints are extensively employed in steel bridges due to their favorable constructability. Furthermore, owing to the prevalence of plate structures, bridges commonly feature numerous non-penetrated fillet weld joints. Under specific conditions, fatigue cracks may initiate from the weld root in non-penetration welded joints, exemplified by the weld between the bottom flange and the sole plate of a bridge.^{3,4} These non-visible fatigue cracks are difficult to detect, yet they exert deleterious effects on the service life of the bridges. Notably, weld root fatigue cracks occur within the structure, so they are impervious to repair or preventive measures through mechanical treatment.⁵⁻⁷ Consequently, precautions must be implemented during the fabrication and construction phases to forestall the occurrence of weld root fatigue cracks in bridges throughout their operational lifecycle.

Numerous studies in the past have extensively investigated visible fatigue cracks. For example, Kiyak et al. provided improved parametric equations for weld toe stress concentration factors and through-thickness stress profiles in butt-welded plates. These equations exhibit extended validity and improved accuracy compared to existing solutions.⁸ Lewandowski and Rozemek et al. conducted fatigue tests on flat specimens with fillet welds, including concave and convex welds. They found that the durability of the specimens with concave welds was slightly higher than that of the specimens with convex welds.^{9,10} In another study, Zhu et al. established a full-scale orthotropic steel bridge deck model. Employing the effective traction structural stress method, they analyzed the most critical loading condition for the failure mode of the rib-to-deck joint under a multiaxial stress state. Their findings indicated that the fatigue failure mode of the rib-to-deck joint was contingent upon the transverse loading locations.¹¹ Furthermore, Wang et al. presented a reliable high-cycle fatigue life assessment method grounded in a unified crack growth approach for welded cruciform joints. Through a comparative analysis with the fatigue life prediction formula in current specifications, they concluded that the latter proved excessively conservative.¹²

Limited attention has been given to non-visible cracks, particularly weld root fatigue cracks, which merit attention. One of the necessary conditions for the occurrence of weld root fatigue cracks is that the weld root

bears substantial cyclic tensile stress. Various factors, including welding defects, residual stress, and loading conditions, can influence the magnitude of cyclic tensile stress at the weld root, impacting the likelihood of fatigue crack formation.^{13,14} To prevent these fatigue cracks, techniques such as assistive bonding have been developed to reduce the cyclic tensile stress applied to the weld root. This method involves inserting an adhesive material (e.g., epoxy) between two steel plates to bond them, followed by welding the plates.¹⁵ Nonnenmann et al. have emphasized the improvement of mechanical properties in hybrid weld-bonded joints.¹⁶ Previous studies have demonstrated that the insertion of epoxy can significantly reduce tensile stress at the weld root. However, welding heat input may cause discoloration or burning of the epoxy, leading to potential welding defects.^{17,18} To address this, this study seeks to reduce welding defects by introducing heat-resistant rubber around the epoxy to prevent its flow. A series of experiments and simulation analyses were conducted to validate the feasibility of this method and assess its effect on weld root fatigue performance.

2 | EXPERIMENTAL PROGRAM

2.1 | Design of specimens

The structure surrounding bridge supports is prone to fatigue and corrosion due to the high-stress state. Welding the bottom flange and the sole plate is limited in its application because it can easily lead to non-visible weld root fatigue cracks. This study aims to explore the feasibility of epoxy bonding-assisted welding technology in preventing root fatigue cracks and enhancing fatigue life. The specimens were designed to simulate the conditions surrounding the bridge support, emphasizing the cyclic tensile stress endured by the fillet weld root between the bottom flange and the sole plate, as illustrated in Figure 1. The details of the specimens are shown in Figure 2. The specimens were 300 mm long, 40 mm wide, and 31 mm high. The flange plate and sole plate were 9 mm and 22 mm thick, respectively. The center of the sole plate was reduced by 0.5 mm thick, and the heat-resistant rubber was inserted around the reduction area to prevent the epoxy from burning and discoloration.¹⁵ The reduced thickness area commenced 15 mm from the weld root. For comparative analysis, specimens without epoxy insertion were also designed. These weld-only specimens, designated as W, incorporated a thickness reduction in the center of the sole plate similar to the other specimens. Specimens combining welding and bonding were designated as WB, and based on the

FIGURE 1 Bridge support. [Colour figure can be viewed at wileyonlinelibrary.com]



Photo from: https://www.mlit.go.jp/chosahokoku/giken/program/kadai/pdf/jusyoy/R4/1_anze1_2.pdf

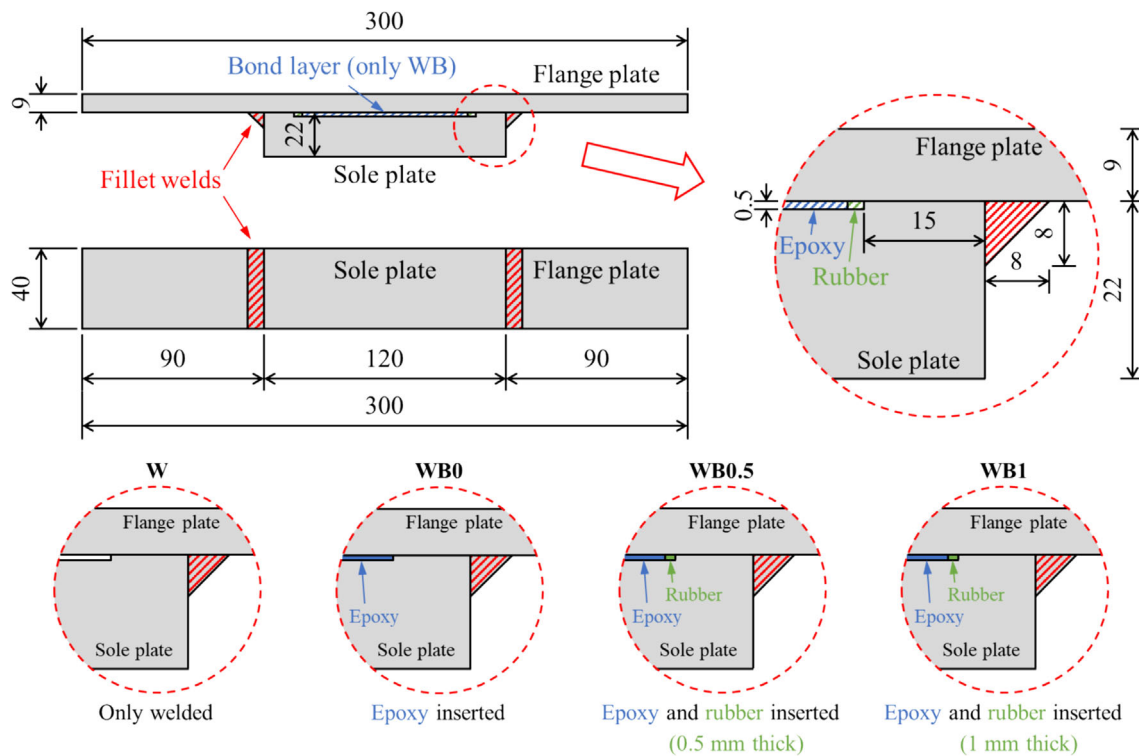
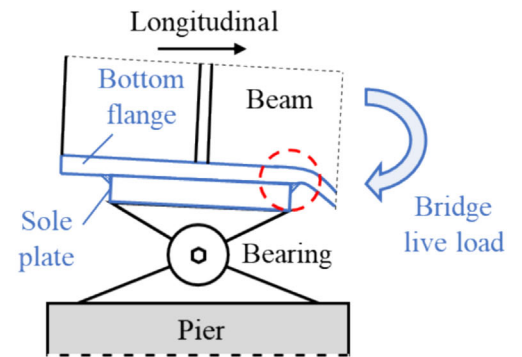


FIGURE 2 Details of specimens (unit: millimeter). [Colour figure can be viewed at wileyonlinelibrary.com]

TABLE 1 Chemical compositions and mechanical properties of steel materials.

| Category | Chemical compositions (mass %) | | | | | Elastic modulus (N/mm ²) | Yield strength (N/mm ²) | Tensile strength (N/mm ²) | Elongation (%) |
|----------------|--------------------------------|------|------|-------|-------|--------------------------------------|-------------------------------------|---------------------------------------|----------------|
| | C | Si | Mn | P | S | | | | |
| SM400A (9 mm) | 0.08 | 0.25 | 0.82 | 0.018 | 0.003 | 2.06×10^5 | 341 | 450 | 31 |
| SM400A (22 mm) | 0.07 | 0.20 | 0.84 | 0.016 | 0.007 | 2.06×10^5 | 290 | 430 | 32 |
| YGW12 | 0.09 | 0.44 | 0.94 | 0.012 | 0.012 | 2.06×10^5 | 460 | 540 | - |

Note: The data of YGW12 are nominal values.

thickness of the inserted rubber, further categorized as WB0 (no rubber), WB0.5 (0.5 mm rubber), and WB1 (1 mm rubber).

The flange plate and sole plate, constructed from SM400A steel, had thicknesses of 9 and 22 mm, respectively. Welding was executed using 1.2 mm diameter

TABLE 2 Mechanical properties of epoxy after heating.

| Heating temperature (°C) | Elastic modulus (N/mm ²) | Tensile strength (N/mm ²) | Tensile lap-shear strength (N/mm ²) |
|--------------------------|--------------------------------------|---------------------------------------|---|
| Unheated | 3800 (25.6) | 35.7 (2.3) | 29.3 (0.6) |
| 150 | 3700 (123.6) | 40.0 (7.1) | 32.4 (1.2) |
| 200 | 2900 (69.9) | 34.2 (6.1) | 32.7 (0.4) |
| 250 | 3100 (119.5) | 38.4 (4.7) | 32.4 (0.3) |

Note: standard deviation.

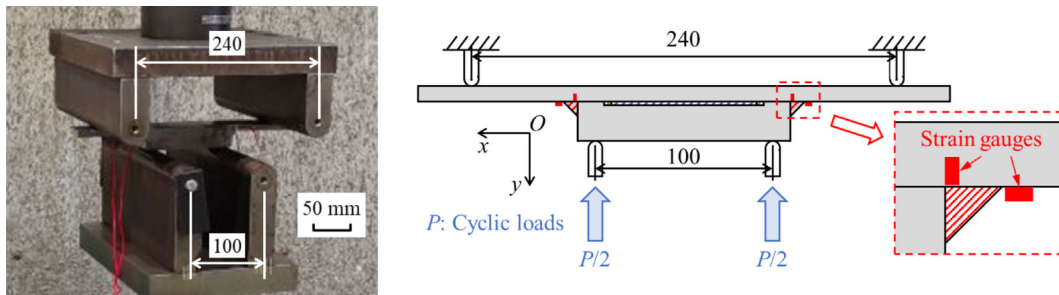


FIGURE 3 Experimental setup (unit: millimeter). [Colour figure can be viewed at [wileyonlinelibrary.com](https://onlinelibrary.wiley.com/doi/10.1111/ffe.14400)]

YGW12 steel wire, classified as a 490 N/mm² class material according to JIS Z3312: 2009 standards.¹⁹ The chemical compositions and mechanical properties of the above steel materials are shown in Table 1. The heat-resistant epoxy resin used was E258R produced by Konishi Chemical Ind. Co., Ltd., and its mechanical properties after heating and cooling are shown in Table 2.

2.2 | Fabrication of specimens

The specimens were classified into four types: W, WB0, WB0.5, and WB1, with each type consisting of nine specimens, resulting in a total of 36 specimens. For the WB specimens, a 0.5-mm thickness reduction was applied to the center of the sole plate using a machining process. Then, both the flange plate and the base plate were heat-treated to eliminate their internal stress. Subsequently, epoxy was evenly spread over the reduced thickness area to bond the flange and sole plate after blasting. Following a 24-h curing period, the flange plate and sole plate were fillet welded using gas metal arc welding. In the case of W specimens, the sole plate also featured a thickness reduction area, and only welding was performed between the flange plate and the sole plate. Welding conditions for all specimens were set at 120 A current, 20 V voltage, and a speed of 5.2 mm/s. Initially, all specimens were fabricated from 200 mm wide steel plates, later cut into individual 40 mm wide specimens. The residual stress was partially released to a lower level during the cutting process, so the residual stress is ignored in the subsequent discussion.

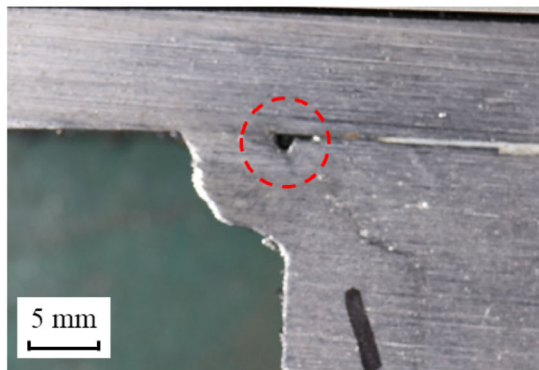
2.3 | Experimental setup

A four-point bending test was performed on the specimens to simulate the applied stress condition of the sole plate of steel bridge supports. The experimental setup is shown in Figure 3. A cyclic load with a frequency of 5 Hz was applied to subject the weld root to tension. The stress ratio according to the nominal stress in the weld roots was set to 0.1. To measure strain near the weld root, two strain gauges (four in total) were affixed to both sides of the flange plate for each specimen. Additionally, a subset of specimens had two extra strain gauges attached near the weld toe at the middle of the flange plate for verification purposes.

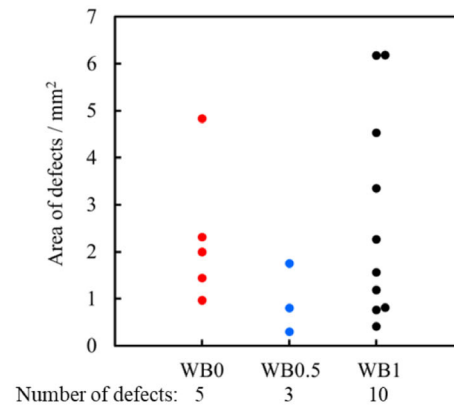
3 | EXPERIMENTAL RESULTS

3.1 | Defects of the specimens

As shown in Figure 4(A), a welding defect attributed to epoxy burning was identified in the weld root. The number and area of welding defects observed in each type of specimen are shown in Figure 4(B). Notably, despite the insertion of rubber, it did not entirely prevent epoxy from flowing out. Welding defects stemming from epoxy burning were evident in some WB specimens. Specifically, WB0.5 specimens exhibited fewer and smaller defects compared to WB0 specimens. Conversely, WB1 specimens displayed the opposite trend, featuring more and larger defects than WB0 specimens. Therefore, inserting



(A) Welding defect



(B) Number and area of welding defects

FIGURE 4 Welding defects attributed to epoxy burning. [Colour figure can be viewed at [wileyonlinelibrary.com](https://onlinelibrary.wiley.com/doi/10.1111/ffe.14400)]

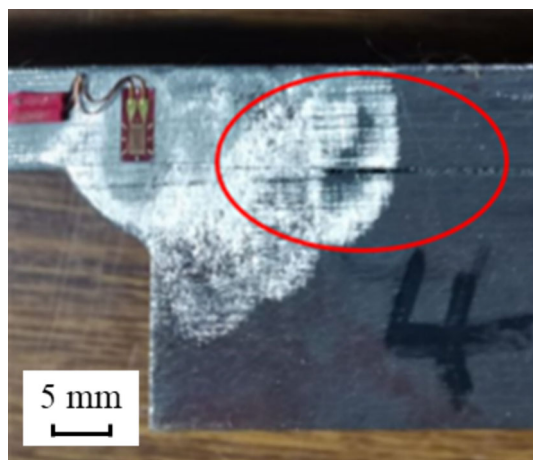


FIGURE 5 Incomplete epoxy filling. [Colour figure can be viewed at [wileyonlinelibrary.com](https://onlinelibrary.wiley.com/doi/10.1111/ffe.14400)]

rubber of appropriate thickness has a positive effect on preventing welding defects. However, excessive rubber thickness may result in a larger gap between the steel plates, causing more epoxy to flow out. Since there are no criteria for this type of welding defect in ISO 5817,²⁰ it is suggested to make an approximate assessment according to the criteria for quality level B, which does not allow incomplete penetration of the weld root. Therefore, all specimens with defects visible to the naked eye were excluded from the subsequent fatigue tests. Furthermore, all WB1 specimens were excluded since they significantly increased the incidence of welding defects. Consequently, the number of specimens used for fatigue tests was reduced to 21, all of which met the requirements of weld quality level B in ISO 5817.²⁰

There was another type of defect that was only found on one WB0 specimen, which is incomplete filling of epoxy as shown in Figure 5. The impact of this type of defect will be discussed later.

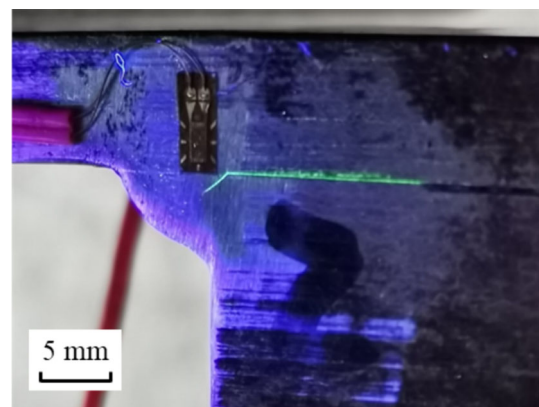


FIGURE 6 Fatigue crack. [Colour figure can be viewed at [wileyonlinelibrary.com](https://onlinelibrary.wiley.com/doi/10.1111/ffe.14400)]

3.2 | Fatigue life

As shown in Figure 6, a fatigue crack was found on the specimen. All cracks identified in this study were brittle cracks and initiated from the weld root. The nominal stress range–fatigue life relationship of all effective specimens is shown in Figure 7(A). Fatigue failure is considered to have occurred when a crack longer than 0.2 mm is observed on the specimen's surface. All fatigue cracks in this study were cracks dominated by mode I. Therefore, to simplify the calculation of the nominal stress range, only the normal stress at the weld root in the y direction ($\sigma_{y,nom}$) was considered. The bonding effect of epoxy and the bending moment in the flange plate were ignored in the calculation, potentially leading to an overestimation of the nominal stress range (Figure 7(B)). Data points marked with arrows signify specimens where no fatigue cracks were detected on the surface, or fatigue failure did not occur even after more than 2 million cyclic loads. The fatigue life of the WB

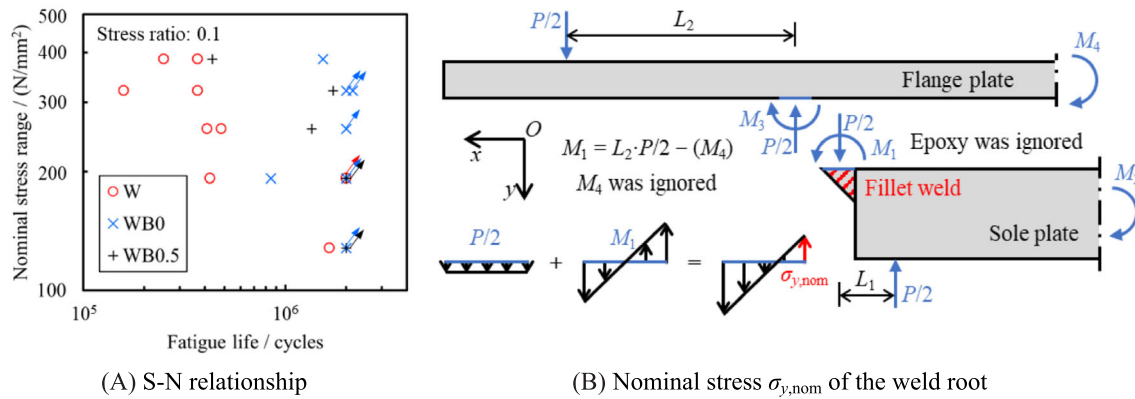


FIGURE 7 S-N relationship. [Colour figure can be viewed at wileyonlinelibrary.com]

specimens was significantly improved compared to the W specimens. For nominal stress ranges exceeding 200 N/mm^2 , WB specimens demonstrated a fatigue life increase of over threefold compared to W specimens. Remarkably, WB specimens with a nominal stress range of approximately 250 to 320 N/mm^2 and W specimens with a nominal stress range of approximately 130 N/mm^2 exhibited comparable fatigue life. This suggests that inserting epoxy can reduce the tensile stress at the weld root by an estimated 50% to 60%. In addition, it is observed that the fatigue lives of WB0.5 specimens were slightly lower than those of WB0 specimens, a phenomenon to be discussed later. However, based on the experimental results, it can be inferred that inserting 0.5 mm thick rubber does not significantly increase fatigue life; its primary role lies in improving welding quality and preventing welding defects. These results were obtained under the condition that the epoxy was not aged. Considering the aging issue of epoxy, further studies are needed to evaluate the long-term effects of applying epoxy.

An exception was noted in the fatigue life of a WB0 specimen with a nominal stress range of 200 N/mm^2 , significantly lower than that of other WB specimens. This discrepancy may be attributed to the incomplete filling of the gap between the two steel plates due to epoxy shrinkage, as shown in Figure 5. To validate this hypothesis, subsequent simulation analyses were conducted.

4 | FINITE ELEMENT ANALYSIS

4.1 | Analysis model

Finite element analysis was performed through the ABAQUS software to investigate the stress distribution near the weld root of the specimens. The analysis model, shown in Figure 8, was configured as one-fourth of the original specimen due to the symmetry. The gap

thickness was set at either 0.2 mm or 0.5 mm based on actual measured results from the specimens. The model employed eight-node solid elements, with a maximum element size of 1 mm. The element size gradually decreased near the weld root, with the minimum size being 0.1 mm. The total number of elements was 131,660, and the total number of nodes was 148,491. Material properties of all three steel materials were the same as the Table 1, and the epoxy properties were set to the data of unheated in Table 2. The Poisson's ratio for steel and epoxy was set at 0.3 and 0.35, respectively. The steel plate and the weld were connected by tie constraints. The normal behavior between the flange and the sole plate was defined as hard contact, and the tangential behavior was defined using the penalty function method with a friction coefficient of 0.3. For WB specimens, the epoxy layer was modeled using solid elements akin to the steel plates, with tie constraints established between the steel plates and the epoxy layer to simulate the bonding effect. A monotonic load equivalent to the load range experienced during experimentation was applied to the model as the general concentrated force on mesh nodes. Residual stresses were ignored in the analysis.

4.2 | Comparison with experimental results

In Figure 9, the strain results derived from the finite element model were compared with the experimentally measured results from strain gauges. The analytical results exhibited strong agreement with the experimental data, affirming the validity of the model. Notably, under identical loads, the strain near the weld root of the WB specimens was reduced by approximately 60% compared to the W specimens. However, the strains near the weld toe for both types of specimens demonstrated similar

FIGURE 8 Analysis model. [Colour figure can be viewed at wileyonlinelibrary.com]

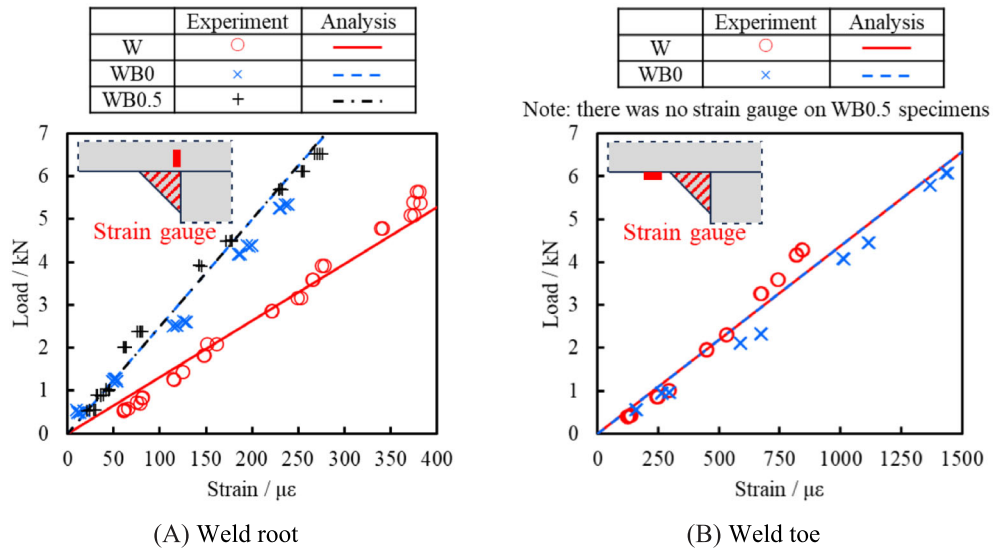
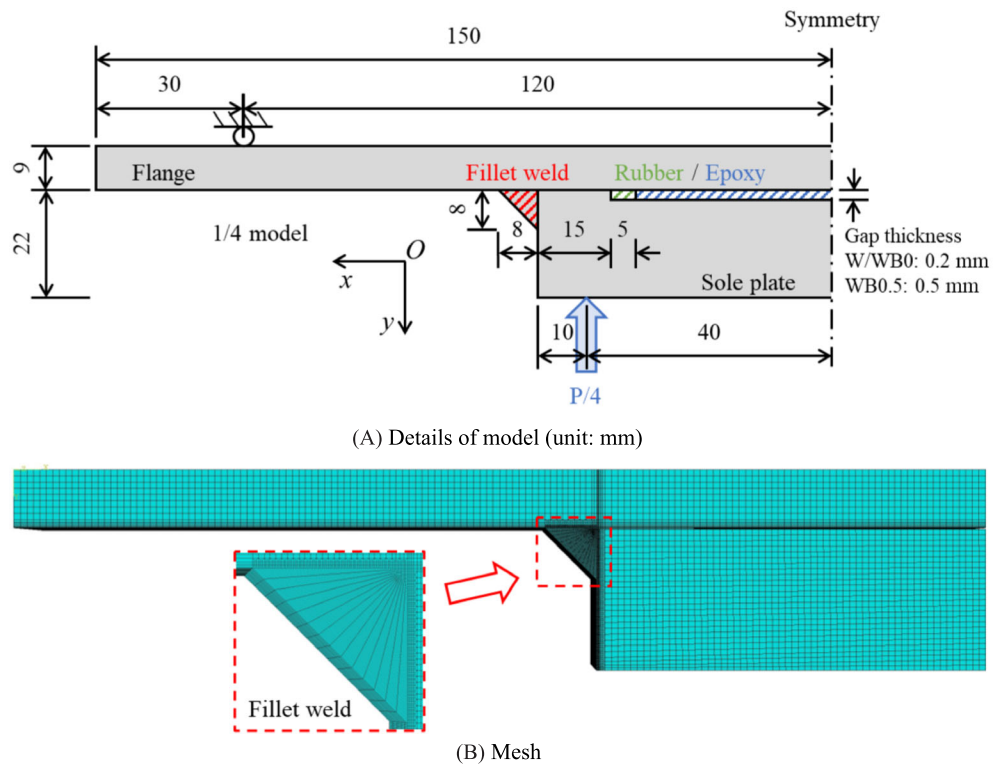


FIGURE 9 Comparison of load-strain relationship. [Colour figure can be viewed at wileyonlinelibrary.com]

magnitudes. This alignment between analytical and experimental results further supports the efficiency of the finite element model in capturing the stress distribution characteristics near the weld root.

4.3 | Stress mitigation

Five load magnitudes corresponding to the experimental conditions were applied in the analysis model. The stress distribution patterns under different load magnitudes

exhibited similarities. Results from a load with a nominal stress range of approximately 250 N/mm² are presented in Figure 10. For all three models (W, WB0, and WB0.5), evident stress concentration at the weld root was observed, with the maximum stress localized at the weld root. The W model exhibited the highest tensile stress. The maximum tensile stresses of both the WB0 model and the WB0.5 model were significantly reduced by about 60% compared with the W model. This is consistent with the previous inference obtained by comparing the fatigue life between W specimens and WB specimens. Moreover,

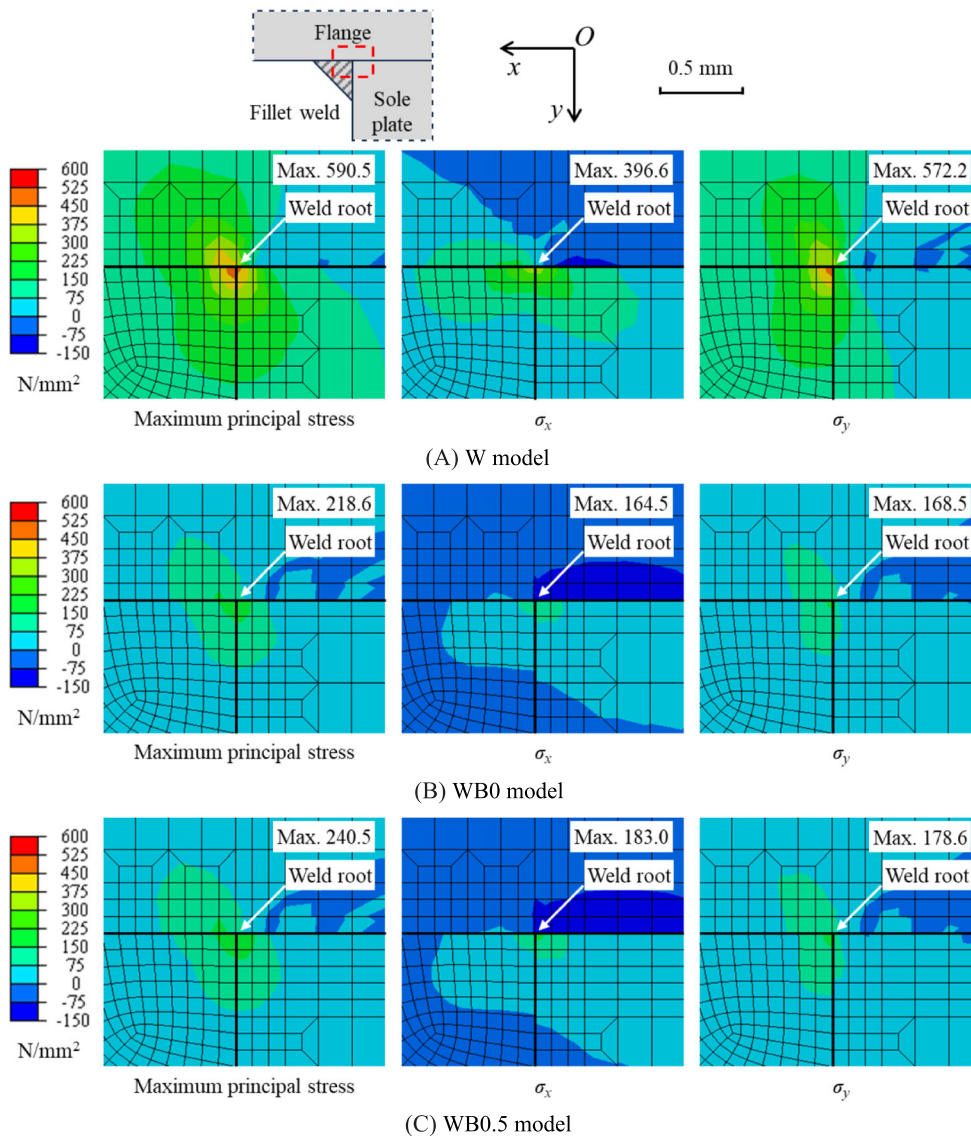


FIGURE 10 Stress distribution around the weld root (unit: N/mm^2). [Colour figure can be viewed at wileyonlinelibrary.com]

it is noteworthy that the insertion of epoxy demonstrated a more pronounced reduction in normal stress in the y direction (σ_y) compared to the x direction (σ_x). The reductions for σ_x and σ_y were approximately 55% and 70% respectively. This emphasizes the effectiveness of epoxy insertion in mitigating tensile stresses, particularly for σ_y .

In addition, the stress distribution patterns of the WB0 model and the WB0.5 model were found to be similar. However, the maximum principal tensile stress of the WB0.5 model was about 10% higher than that of the WB0 model. This concurs with the experimental results depicted in Figure 7, indicating slightly lower fatigue lives for WB0.5 specimens compared to WB0 specimens. A plausible explanation for this discrepancy lies in the insertion of rubber, which potentially increased the gap between the two steel plates in WB0.5 specimens compared to WB0 specimens. Consequently, the epoxy layer in WB0.5 specimens was thicker than that in WB0

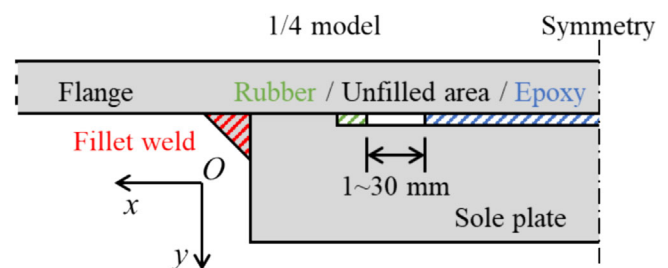


FIGURE 11 Analysis model with defect. [Colour figure can be viewed at wileyonlinelibrary.com]

specimens. Given that the elastic modulus of epoxy is significantly smaller than that of steel, a thicker epoxy layer exerts a lesser constraining effect on the steel plates. During modeling, gap thicknesses were set at 0.2 and 0.5 mm for WB0 and WB0.5 specimens, respectively, following measured results, as shown in Figure 8(A).

4.4 | Incomplete epoxy filling

As mentioned in Section 3.2, a WB0 specimen with incomplete epoxy filling was identified, leading to a markedly reduced fatigue life compared to other WB specimens. To investigate this hypothesis, finite element models were established to simulate defects. As shown in Figure 11, the gap between the two steel plates was not entirely filled with epoxy. It is assumed that the length of the unfilled area is consistent across the specimen width, with lengths varying from 1 to 30 mm. All other details of the model remain consistent with Figure 8.

Under a load with a nominal stress range of approximately 250 N/mm^2 at the weld root, the models were analyzed to determine the maximum principal stress at the weld root for various defect lengths, as shown in Figure 12. The maximum principal stress at the weld root increased with the defect length in both WB0 models and WB0.5 models. In the case of large defects, the increase in the maximum principal stress at the weld root with

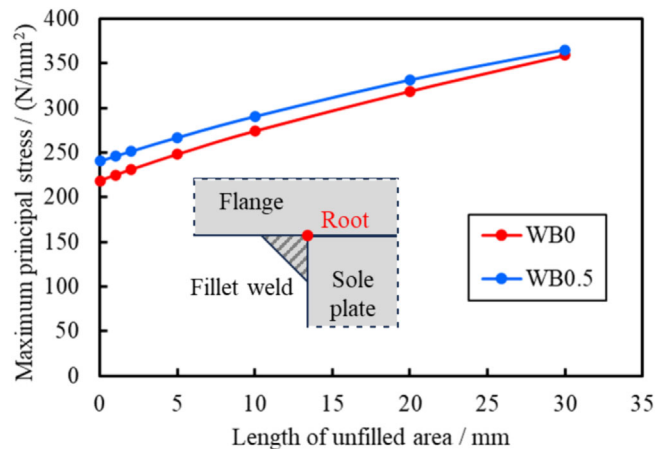


FIGURE 12 Maximum principal stress of weld root. [Colour figure can be viewed at wileyonlinelibrary.com]

the defect length was smaller than that of small defects. Furthermore, in the case of small defects, the maximum principal stress at the weld root differed by about 10% between the WB0 models and WB0.5 models. However, when the defect length reached 30 mm, the results of the two models were almost consistent. This observation indicates that the discrepancy in maximum principal stress between WB0 and WB0.5 models is primarily attributed to the differing thickness of the epoxy layer, rather than variations in the gap thickness between the flange and sole plate.

5 | DISPLACEMENT-BASED FATIGUE STRENGTH EVALUATION

In engineering, the conventional approach to evaluating fatigue strength involves utilizing the S-N relationship, which establishes a link between fatigue strength and fatigue life. However, due to the particularity of the weld root, it is difficult to measure its stress. Nominal stress, commonly used for evaluation, fails to capture stress concentration at the weld root. Even with finite element analysis, due to the stress singularity at the weld root, the stress magnitude is susceptible to influences such as element type, element size, and mesh method.²¹ Obtaining precise stress results often necessitates extensive experience and multiple attempts. While the notch stress approach eliminates stress singularities to a certain extent, it will augment the modeling workload, particularly in models housing numerous stress singularities. Furthermore, this approach also needs to adjust the size of the notch with structures of varying dimensions based on empirical insights.^{22–24} In response to these issues, Tateishi et al. proposed a displacement-based method for evaluating the fatigue strength of weld roots. This method, relying on displacement, is less affected by mesh-related uncertainties, thereby yielding relatively

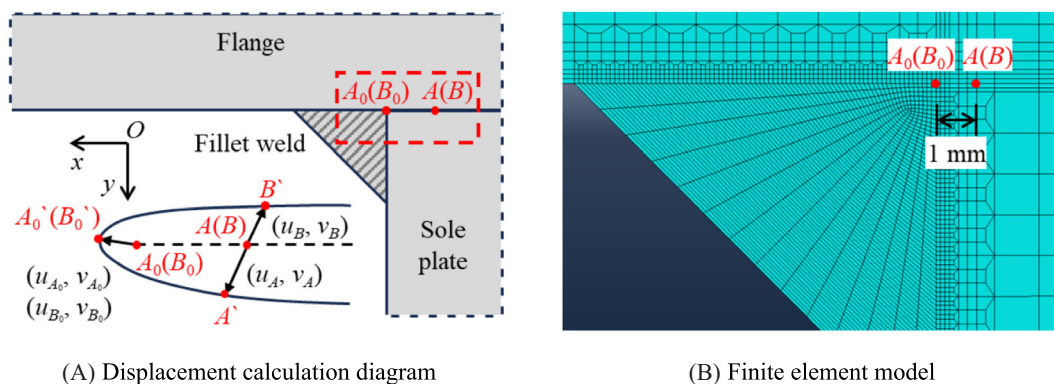


FIGURE 13 Calculation of displacement near weld root. [Colour figure can be viewed at wileyonlinelibrary.com]

stable results.²⁵ Moreover, the model can be established to mirror the actual structural configuration, rendering it more efficient and intuitive. Therefore, this displacement-based method was employed in this study to analyze the improvement of fatigue strength of weld roots achieved by inserting epoxy and rubber.

5.1 | Calculation of displacement

As shown in Figure 13, four nodes are selected near the weld root for calculating displacement. A_0 and B_0 are positioned at the weld root, and A and B are in the unwelded part, 1 mm away from the weld root. A is situated on the sole plate, and B is on the flange. The displacement components u and v represent the displacement in the x direction and y direction, respectively.

Excluding the influence of the elastic deformation at the weld root, the displacement components u and v are calculated by the following formulas:

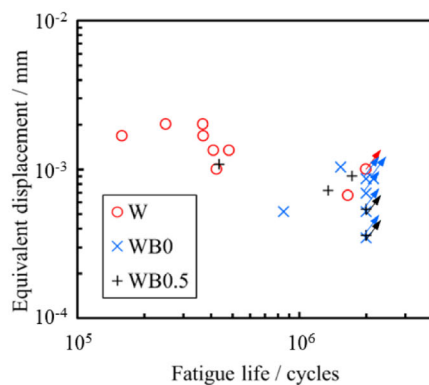
$$u = |(u_A - u_{A0}) - (u_B - u_{B0})| \quad (1)$$

$$v = |(v_A - v_{A0}) - (v_B - v_{B0})| \quad (2)$$

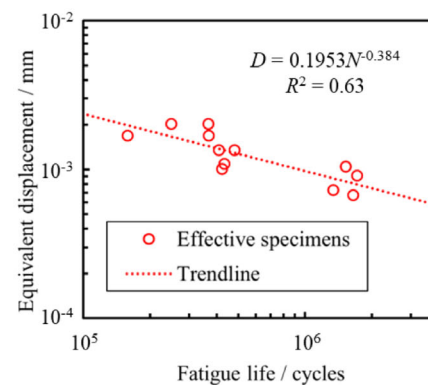
where u_A , u_{A0} , u_B , and u_{B0} are the displacements of A , A_0 , B , and B_0 in the x direction, respectively; v_A , v_{A0} , v_B , and v_{B0} are the displacements of A , A_0 , B , and B_0 in the y direction, respectively. Notably, the gap between the flange and sole plate at the weld root is 0 mm, so $u_{A0} = u_{B0}$ and $v_{A0} = v_{B0}$.

The displacement components u and v correspond to load mode II and mode I, respectively. The equivalent displacement d is given by the following formula:

$$d = \sqrt{3u^2 + v^2} \quad (3)$$



(A) D-N relationship



(B) Fatigue life prediction by D-N relationship

5.2 | D-N relationship

The relationship between the fatigue life and the equivalent displacement of all specimens is plotted in Figure 14 (A). Notably, the equivalent displacements of WB specimens were generally smaller than those of W specimens. This observation suggests that inserting epoxy effectively limits the deformation of the weld root, thereby enhancing its fatigue life. This finding aligns with the conclusions drawn from fatigue assessments using stress, reinforcing the efficiency of epoxy insertion in improving weld root performance.

Compared with Figure 7(A), it is evident that all data points in Figure 14(A) exhibit a more pronounced concentration. A trendline was fitted to the dataset comprising effective specimens, excluding those specimens without detected fatigue cracks or with incomplete epoxy filling, as shown in Figure 14(B). This trendline, herein referred to as the D-N relationship, bears a resemblance to the conventional S-N relationship. The correlation coefficient between the experimental results and the trendline was calculated to be 0.63, surpassing the 0.10 correlation coefficient obtained when employing nominal stress fitting. Therefore, it can be considered that this method can effectively evaluate the fatigue strength of the weld root. Further, it can effectively evaluate the improvement of weld root fatigue performance by inserting epoxy.

6 | CONCLUSIONS

This study experimentally investigated the influences on the welding quality and the fatigue performance of fillet weld root by inserting adhesive material of epoxy between the flange and sole plate. All the tests were repeatable. Simulation analyses were further conducted to investigate the stress distribution near the fillet weld

FIGURE 14 Equivalent displacement–fatigue life relationship. [Colour figure can be viewed at [wileyonlinelibrary.com](https://onlinelibrary.wiley.com)]

root and the impact of incomplete epoxy filling on the stress at the weld root. The fatigue strength evaluation of specimens in this study utilized the displacement-based method. The following conclusions were obtained.

1. Welding heat input can result in epoxy burning and gas production, leading to welding defects. The experimental results indicate that using 0.5 mm thick heat-resistant rubber around the epoxy minimizes welding defects due to epoxy burning. Specimens with 0.5 mm rubber (WB0.5) exhibited fewer and smaller defects compared to those with no rubber (WB0) or thicker rubber (WB1). Although WB0.5 did not improve fatigue life compared to WB0, it had better welding quality. This provides the possibility for applying epoxy bonding-assisted welding in engineering.
2. According to experimental and analytical results, inserting epoxy can significantly reduce the maximum principal tensile stress at the weld root. Under four-point bending load conditions, the maximum principal tensile stress can be reduced by approximately 60%. Furthermore, it can reduce both the normal stress in the x direction (σ_x) and the y direction (σ_y) by about 55% and 70% respectively. Since the elastic modulus of epoxy is much smaller than that of steel, a thicker epoxy layer has a weaker constraining effect on the flange and sole plate than a thinner one. Therefore, inserting a thick epoxy layer results in less effective stress reduction at the weld root than inserting a thin one. Moreover, incomplete epoxy filling resulted in a larger maximum principal stress at the weld root than complete filling. Additionally, stress magnitude increased with the length of the unfilled area.
3. The equivalent displacement method is more suitable for evaluating the fatigue strength of fillet weld roots under bending and shear loads and assessing the improvements achieved by epoxy insertion compared to the nominal stress method. The D-N relationship, based on equivalent displacement, exhibited a better concentration of experimental data compared to the S-N relationship based on the nominal stress range. The correlation factor for the fitted D-N relationship of effective specimens reached 0.63, indicating its effectiveness in fatigue strength evaluation.

This study was conducted under the ideal condition that the epoxy resin had not aged. Considering the long service life of engineering structures, the long-term effect and the degradation mechanism of epoxy bonding-assisted welding need further study.

AUTHOR CONTRIBUTIONS

Experiment: J. Mao, Y. Xu; analysis: J. Mao, Y. Xu; methodology: M. Hirohata, K.-H. Chang; validation: M. Hirohata; investigation: M. Hirohata, K.-H. Chang; writing: J. Mao; review and editing: M. Hirohata, K.-H. Chang.

All authors have read and agreed to the published version of the manuscript.

CONFLICT OF INTEREST STATEMENT

The authors declare no conflicts of interest.

DATA AVAILABILITY STATEMENT

The data that support the findings of this study are available from the corresponding author upon reasonable request.

NOMENCLATURE

| | |
|-----------------------------------|---|
| P | nominal load range |
| M_1 | bending moment transmitted from flange to weld |
| M_2 | bending moment in the sole plate |
| M_3 | bending moment transmitted from weld to flange |
| M_4 | bending moment in the flange plate |
| L_1 | distance from the loading line on the sole plate to 1/2 weld leg in the x direction |
| L_2 | distance from the loading line on the flange plate to 1/2 weld leg in the x direction |
| $\sigma_{y,nom}$ | nominal normal stress in the y direction |
| σ_x | normal stress in the x direction |
| σ_y | normal stress in the y direction |
| A, A' | node on the sole plate 1 mm away from the weld root before and after deformation |
| A_0, A_0' | node on the sole plate at the weld root before and after deformation |
| B, B' | node on the flange 1 mm away from the weld root before and after deformation |
| B_0, B_0' | node on the flange at the weld root before and after deformation |
| u | displacement component in the x direction |
| $u_A, u_{A_0}, u_B,$ u_{B_0} | displacements of $A, A_0, B,$ and B_0 in the x direction |
| v | displacement component in the y direction |
| $v_A, v_{A_0}, v_B,$ v_{B_0} | displacements of $A, A_0, B,$ and B_0 in the y direction |
| d | equivalent displacement |
| S | stress |
| D | displacement |
| N | number of cycles to failure |
| R^2 | correlation coefficient |

ORCID

Mao Jiahao  <https://orcid.org/0000-0001-5303-6662>

REFERENCES

- Haghani R, Al-Emrani M, Heshmati M. Fatigue-prone details in steel bridges. *Buildings*. 2012;2(4):456-476.
- Presno Vélez Á, Bernardo Sánchez A, Bruna OA, Abella DM, de Prado LÁ, Fernández MM. Material behavior and fatigue assessment of old steel bridges of the Spanish conventional rail network. *Materials*. 2021;14(18):5275.
- Fricke W, Kahl A, Paetzold H. Fatigue assessment of root cracking of fillet welds subject to throat bending using the structural stress approach. *Weld World*. 2006;50(7-8):64-74.
- Alencar G, de Jesus A, da Silva JGS, Calçada R. Fatigue cracking of welded railway bridges: a review. *Eng Fail Anal*. 2019;104:154-176.
- Ghanem F, Fredj NB, Sidhom H, Braham C. Effects of finishing processes on the fatigue life improvements of electro-machined surfaces of tool steel. *Int J Adv Manuf Technol*. 2011;52(5-8):583-595.
- Qu S, Duan C, Hu X, Jia S, Li X. Effect of shot peening on microstructure and contact fatigue crack growth mechanism of shaft steel. *Mater Chem Phys*. 2021;274:125116.
- Al-Karawi H, Al-Emrani M. Fatigue life extension of existing welded structures via high frequency mechanical impact (HFMI) treatment. *Eng Struct*. 2021;239:112234.
- Kiyak Y, Madia M, Zerbst U. Extended parametric equations for weld toe stress concentration factors and through-thickness stress distributions in butt-welded plates subject to tensile and bending loading. *Weld World*. 2016;60(6):1247-1259.
- Lewandowski J, Rozumek D. Fatigue crack growth in welded S355 samples subjected to bending loading. *Metals*. 2021;11(9):1394.
- Rozumek D, Lewandowski J, Lesiuk G, Marciniak Z, Correia JA, Macek W. The energy approach to fatigue crack growth of S355 steel welded specimens subjected to bending. *Theor Appl Fract Mech*. 2022;121:103470.
- Zhu Y, Deng C, Gong B, et al. Fatigue failure modes of rib-to-deck joints under the multiaxial stress states caused by various wheel loading characteristics. *Fatigue Fract Eng Mater Struct*. 2023;46(1):111-124.
- Wang W, Shi W, Li B, Mi Z. *High-cycle fatigue life assessment of welded cruciform joints of Q460D steel*. Structures. Vol. 57. Elsevier; 2023:105163.
- Lawrence FV, Munse WH. Fatigue crack propagation in butt welds containing joint penetration defects. *Weld J*. 1973;52:221s.
- Zerbst U, Hensel J. Application of fracture mechanics to weld fatigue. *Int J Fatigue*. 2020;139:105801.
- Hirohata M. Static tensile strength characteristics of fillet welding lap joints assisted with bonding. *Weld Int*. 2016;30(1):9-17.
- Nonnenmann T, Beygi R, Carbas RJ, da Silva LF, Öchsner A. Synergetic effect of adhesive bonding and welding on fracture load in hybrid joints. *J Adv Join Process*. 2022;6:100122.
- Mikihito H, Yoshito I. Fatigue characteristics of patch plate joints by fillet welding assisted with bonding. *Weld Int*. 2018;32(4):243-253.
- Xu Y, Hirohata M, Suzuki T, Konishi H, Tominaga S. Assistive bonding assisted prevention of weld root fatigue cracks. *Q J Jpn Weld Soc*. 2022;40(4):5WL-8WL.
- Japanese Industrial Standards Committee. Solid wires for MAG and MIG welding of mild steel, high strength steel and low temperature service steel, JIS Z 3312: 2009.
- International Organization for Standardization. welding - fusion-welded joints in steel, nickel, titanium and their alloys (beam welding excluded) - Quality levels for imperfections, Fourth edition, ISO 5817:2023.
- Bartsch H, Citarelli S, Feldmann M. Generalisation of the effective notch stress concept for the fatigue assessment of arbitrary steel structures. *J Constr Steel Res*. 2023;201:107715.
- Fricke W. Guideline for the fatigue assessment by notch stress analysis for welded structures. 2008; IIW, 13, 2240-08.
- Sonsino CM, Fricke W, De Bruyne F, Hoppe A, Ahmadi A, Zhang G. Notch stress concepts for the fatigue assessment of welded joints—background and applications. *Int J Fatigue*. 2012;34(1):2-16.
- Fricke W. IIW guideline for the assessment of weld root fatigue. *Weld World*. 2013;57(6):753-791.
- Tateishi K, Soda N, Hanji T, Shimizu M. Displacement based fatigue strength evaluation for root failure in fillet weld joints. *J JSCE, Ser A1*. 2015;71(3):315-326. (in Japanese)

How to cite this article: Jiahao M, Mikihito H, Yifei X, Kyong-Ho C. Fatigue performance of bonding-assisted fillet weld roots by inserting adhesive material. *Fatigue Fract Eng Mater Struct*. 2024;1-12. doi:10.1111/ffe.14400